

# Intelligent Application of Photogrammetry in Computer Reverse Modeling of Building Structural Engineering

Yuqing Liu, Yue Gao\*, Fengjuan Guo, Xiangyu Jia

Hebei University of Water Resources and Electric Engineering, 061001, Cangzhou, Hebei, China

E-mail: yuqingliu26@163.com; yuegao227@163.com; fengjuanguo7@163.com; xiangyujia2@126.com

\*Corresponding author

**Keywords:** photogrammetry, building structure, computer, backward modeling

**Received:** March 14, 2024

*This paper addresses the challenge of insufficient elevation data in building modeling obtained through oblique photogrammetry. It explores the application of close-range oblique photogrammetry for reverse modeling in building structural engineering. The methodology employs a DJI Phantom 4 Pro UAV, equipped with a tilt camera on the flight control platform, to capture image data. Checkpoints were established on the keel frame to evaluate the accuracy of the 3D model. Experimental results show that the discrepancies between measured and model distances range from a maximum of 0.006m to a minimum of 0.003m, with height measurement differences varying from 0.005m to 0.002m. These results demonstrate millimeter-level accuracy, highlighting the method's high geometric precision. The UAV tilt photogrammetry method was validated for practical applications, meeting the requirements for detailed individual building modeling. It provided high-resolution facade textures and proved effective for producing geometrically accurate models suitable for structural engineering purposes.*

*Povzetek: Članek uporablja fotogrametrijo z inteligentnimi algoritmi za povratno modeliranje v gradbenem inženirstvu, izboljšuje kvaliteto 3D modelov s pomočjo UAV-jev in naprednih metod za obdelavo slik.*

## 1 Introduction

The so-called reverse engineering technology refers to the spatial measurement of objects or models by certain measuring means, and the process of reverse engineering technology is very different from traditional forward design, which reconstructs CAD models through a 3D geometric modeling method based on the measured data [1]. Reverse engineering starts with the prototype of the product and then obtains the 3D digital model of the product so that it can be further processed by advanced technology such as CAD, ACE, CAM, and CIMS. Reverse engineering technology provides very good technical support for rapid design and manufacturing. It has become one of the most important and concise methods of information transmission in the manufacturing industry. In the design of reverse engineering technology, it is necessary to extract 3D spatial data information from design objects. The development of detection equipment provides hardware conditions for obtaining 3D information on products [2].

The detection equipment of reverse engineering technology includes three coordinate measuring machines and three-dimensional scanners produced in Britain, Italy, Germany, Japan, and other countries. The probe's structure principle divides it into two kinds: contact and non-contact. The contact probe can further be divided into two kinds: hard probe and soft probe. The contact probe and the measured object directly contact each other to obtain data [3]. The non-contact probe applies the optics or laser principal implementation strategy. The CYCLON2 high-speed scanner from the British Renishaw

company can realize the interchange of laser probe and contact scanning heads with laser probe scanning accuracy up to 0.05mm and contact scanning probe accuracy up to 0.02mm. GOM's ATOS scanner, a German company, can freely move around the object being measured and acquire surface data using the light band through the data image processor [4].

The scanning range can be up to 8 m. The PIX-30 dot contact scanner of Roland Company in Japan, the TALYSCAN 150 multi-sensor scanner of Taylor Hopson Company in Britain, etc., embodies the characteristics of high speed, low price, and functional compound of testing equipment and provide a good hardware condition for the realization of CAD/CAE/CAM integration from the physical-mathematical model [5]. The motivation behind this research stems from the critical need to address the challenges associated with insufficient elevation data in building modeling, particularly in the context of oblique photogrammetry. Existing methodologies may fall short of delivering accurate and detailed representations of building structures, emphasizing the demand for innovative approaches to enhance modeling precision. This study contributes to the field by investigating the application of oblique photogrammetry in reverse modeling, specifically within the realm of close-range photogrammetry for building structural engineering. The findings presented in this paper offer valuable insights into the accuracy and geometric precision achievable through the utilization of unmanned aerial vehicle tilt photogrammetry. By looking at the differences between measured distances and model representations, this study adds to our understanding of how well the method works

and lays the groundwork for improving individual modeling needs with more detailed facade textures and higher resolution.

In recent years, the demand for accurate and efficient building modeling has intensified, particularly in the fields of structural engineering and architectural design. Traditional modeling techniques often fall short in capturing complex geometries and elevations, necessitating innovative approaches to enhance accuracy and efficiency. This study explores the application of oblique photogrammetry using consumer-grade unmanned aerial vehicles (UAVs) for reverse modeling of buildings. By leveraging the capabilities of UAV tilt photogrammetry, this research addresses the critical challenge of inadequate elevation information and the limitations of existing photogrammetry methods. The motivation behind this research stems from the growing need for high-precision modeling in the construction industry, where traditional methods struggle to meet accuracy demands. The integration of UAV technology in photogrammetry presents an opportunity to overcome these limitations, offering enhanced data acquisition and processing capabilities. This study contributes to the field by presenting a novel methodology that combines UAV tilt photogrammetry with advanced data processing techniques, demonstrating its effectiveness in accurately modeling building structures. We provide detailed insights into the UAV flight patterns, data acquisition process, and statistical analysis of results, establishing a framework for future applications in building modeling and construction measurement. The paper is organized as follows: Section 2 provides a comprehensive literature review, highlighting existing photogrammetry methods and their limitations. Section 3 details the methodology employed in the research, including the UAV setup and data processing techniques. Section 4 presents the experimental results and analysis. Section 5 concludes the paper, offering suggestions for future research directions.

## 2 Literature review

Yang *et al.*, have established a fall hazard management system at the construction site. The system uses computer vision instead of a sensor system as a bridge for information exchange between physical construction sites and virtual models [6]. The main purpose of Jasim *et al.*, is to propose a conceptual model that combines the basic principles of knowledge management with the contemporary principles of BIM at the design stage. This model can store, classify, and share the knowledge generated in past designs into future projects [7]. Liu *et al.*, took the tomb murals as the research object and realized the development of the Tang Dynasty tomb mural clothing patterns and the 3D simulation repair of clothing through 3D interactive clothing pattern production technology and virtual simulation technology [8]. The development of effective models for image categorization has been the main focus of related work on the subject. Jang *et al.*, presented a deep learning method that achieved great accuracy but had a processing overhead [9]. Bartonek and Buday presented a transfer learning method

that improved model generalization [10]. On the other hand, Camagni *et al.*, stressed the significance of feature engineering, leading to enhanced accuracy [11]. These studies, however, don't provide a thorough assessment of processing speed. Furthermore, Tiwari *et al.*, introduced a model that prioritizes real-time processing at the expense of accuracy [12]. To address these gaps, we propose a model that excels in both processing speed and accuracy. In recent years, the measuring field in our country has introduced and developed digital photogrammetry. Computer technology, pattern recognition, and other multidisciplinary theories and methods apply digital image matching to extract the geometric and physical information of the objects taken digitally, based on the basic principles of digital image and photogrammetry. Abroad, it is called softcopy photogrammetry, while in our country, it is referred to as full digital photogrammetry. This definition holds that in the process of digital photogrammetry, not only the product is digital, but also the recording of intermediate data and the raw data processed are digital [13]. GSI, USA developed the V-STARS (Video-Simultaneous Triangulation and Resection System) system, which serves as the representative product of digital photogrammetry technology. The system mainly has the advantages of high 3D measurement accuracy (relative accuracy up to 1/20 million), fast measurement speed, a high degree of automation, and the ability to work in harsh environments (such as thermal vacuums). It is currently the most mature commercial industrial digital photogrammetry product in the world [14].

Despite the advancements in photogrammetry, traditional methods often struggle to capture accurate elevation data, especially in complex building structures. Existing techniques primarily rely on ground-based data collection, which can be time-consuming and may yield limited results in terms of geometric precision. Recent studies have explored the use of unmanned aerial vehicles (UAVs) in photogrammetry, demonstrating their potential to enhance data acquisition efficiency and accuracy. However, there remains a gap in the literature regarding the systematic application of UAV tilt photogrammetry for reverse modeling, particularly in close-range scenarios relevant to building structural engineering. This research aims to fill this gap by employing a consumer-grade UAV equipped with tilt cameras, enabling detailed and accurate modeling while addressing the limitations of traditional approaches. The prevailing challenge in contemporary building modeling lies in the inadequacies of elevation information acquired through oblique photogrammetry. Existing methodologies often encounter limitations in delivering accurate representations of building structures, leading to a pronounced need for a more robust and precise approach to overcome these shortcomings. However, there is a significant research gap in exploring oblique photogrammetry for reverse modeling in the context of close-range photogrammetry for building structural engineering. This study aims to bridge this gap by scrutinizing the effectiveness of unmanned aerial vehicle tilt photogrammetry, particularly in addressing the specific challenges associated with individual modeling

requirements. To address the aforementioned challenges, this research adopts a comprehensive methodology involving unmanned aerial vehicle tilt photogrammetry. Leveraging close-range photogrammetry principles, the study conducts experiment in building structural engineering. The evaluation of measured plane distances and model distances, alongside height measurements, serves as the cornerstone for assessing the accuracy and geometric precision achievable through the proposed methodology.

### 3 Close photogrammetry

#### 3.1 Construction measurement method of building accessory facilities based on UAV

The construction measurement of accessory facilities based on UAV is divided into two parts: field data acquisition and internal data processing (Figure 1). The tilt photogrammetry system of UAV mainly includes three parts: tilt camera of flight control platform and flight data processing software. Uav can be divided into consumer UAV and professional UAV according to operation purposes, and multi-rotor UAV and fixed wing according to wing form. Among them, multi-rotor consumer UAV is low in price and small in size. The advantages of strong mobility and flexibility have been widely used. The multi-rotor consumer UAV can enter some areas with difficult operating conditions, collect image data information that cannot be obtained by conventional methods, and then quickly establish an intuitive and reliable 3D real model, providing geographic information data for engineering construction or other related work of urban management [15].

#### 3.2 UAV field data acquisition

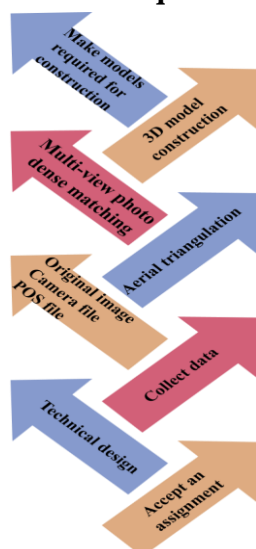


Figure 1: Flow chart of building ancillary facilities measurement based on UAV

According to different building ancillary facilities, different types and categories of UAV equipment are adopted. In this experiment, DJI consumer quadrotor UAV Phantom 4 Pro is adopted. The UAV is stable, safe and flexible, and has a line-of-sight prompt system, GPS positioning system and IMU inertial navigation system, and POS data in the photos taken. The UAV is equipped with a camera with a field Angle of  $84^\circ$  and an effective pixel of 20 million, equivalent to a 35 mm camera with a standard focal length of  $f/2.8 \sim f/11$  and a pin-top camera with autofocus. Due to the complex surrounding environment of the ancillary facilities of the building, in order to make the data sufficient and ensure the safety of the equipment, the vertical flight path is matched with 70%~80% heading and side overlap degree to ensure the image data quality, and the data is collected at a distance of about 3 m close to the ancillary facilities. Before image data acquisition, several checkpoints were set on the keel frame to evaluate the accuracy of the 3D model [16].

#### 3.3 Construction of 3D model of building ancillary facilities

The multi-angle mm photo data with high overlap rate were collated and checked, and then 3D modeling software was used for fine construction of the target model. The data processing mainly included the steps of photo preprocessing, aerial triangulation, multi-view image intensive matching and 3D product model construction.

##### 3.3.1 Aerial triangulation and addition of model scale information

Aerial triangulation, also known as air-three encryption, is a process of calculating the coordinates of other required encryption points through the measured image points on the photo based on a rigorous mathematical model in photogrammetry. It is a key part of the industry processing of UAV images. The tilting photogrammetry system takes the original POS data as the initial parameter, combines the camera file and image information, and extracts the corresponding feature points on each pyramid image through the automatic pyramid matching mode from coarse to fine, and uses the same name connection points on each image to carry out the global area network beam adjustment, and obtains the matching results of the same name points [17]. At the same time, in order to ensure the adjustment accuracy, the internal processing flow of multi-view image joint solution of connection point control point and IMU auxiliary data is established, as shown in Figure 2.

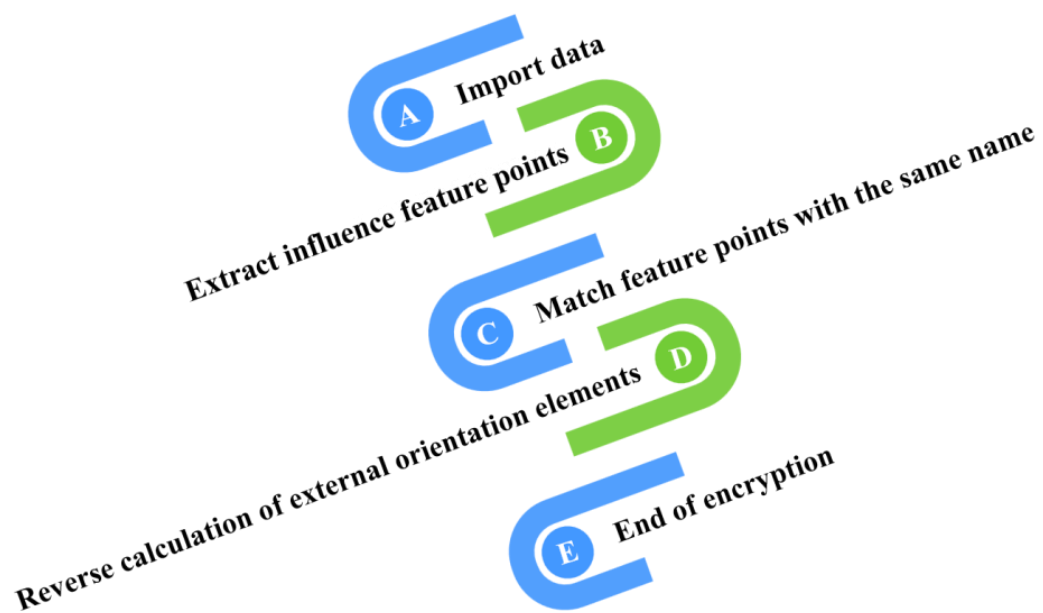


Figure 2: Geolord-AT three-dimensional triangulation process

The proposed study involves a systematic processing workflow to ensure high accuracy in 3D modeling through UAV tilt photogrammetry. Initially, the UAV, equipped with a tilt camera, is deployed to capture image data from various angles during the flight, ensuring adequate overlap for comprehensive coverage of the building structure. Following data acquisition, the images are imported into specialized photogrammetry software, where they undergo alignment and aerial triangulation to create a dense point cloud. This point cloud is then processed to generate a textured 3D model, leveraging advanced image-matching techniques and software configurations to optimize data quality. Finally, checkpoints placed on the building structure are utilized to validate the accuracy of the generated model by comparing measured distances with the model distances, ensuring compliance with relevant standards and enhancing the model's geometric precision. To ensure the robustness of the model, specific parameters for aerial triangulation, such as ground control points and image-matching thresholds, are meticulously defined. The model is validated using checkpoints placed on the building structure, where measured distances are compared with model distances to evaluate accuracy. Statistical analyses are performed to assess the model's precision and identify potential sources of error, enhancing the reliability of the results. This thorough processing methodology not only meets relevant industry standards but also contributes to the creation of highly detailed and accurate models, significantly advancing the field of building structural engineering.

In this Smart-3D software, the most rigorous and accurate regional network adjustment method of beam method is adopted. The collinear equation of the center projection is taken as the basic equation of adjustment, and the photographic beam is taken as the basic unit to achieve the best intersection of the beams between the models, so as

to obtain the ground coordinates and external elements of the encrypted points. The image data is imported into the Smart-3D software to automatically carry out air-three encryption and obtain the position and attitude Angle information of each image [18].

According to the checkpoint set in field data acquisition, according to the spatial distribution of each checkpoint, the appropriate checkpoint is selected as the scale identification point (A, B, C) on the photo, and the puncture point is used as the scale constraint point. a, b, c, and the distance between constraint points is set according to the actual distance of field measurement. Other checkpoints can be used as points to check the accuracy of the model.

### 3.3.2 Multi-view image intensive matching

The field data acquired by UAV includes aerial photography data from multiple perspectives. The multi-view image intensive matching technology is the key technology to study these data. The principle of image matching is to determine the same name points between images by correlation function according to the similarity between multiple images. The main process of image matching is to obtain the external elements of the image and classify the images with accurate external elements. Then the classification results were matched to obtain high high-density point cloud. Finally, the 3D point cloud with high precision is obtained by filtering. Multi-view image intensive matching technology can make better use of redundant image information, combine the POS data of each image and other information, reasonably use multi-view data required by multi-view matching accurately obtain the same name coordinates of multi-view image points, and then obtain the final three-dimensional data information of buildings [19].

### 3.3.3 Three-dimensional product model construction

The dense point cloud generated based on the multi-view image intensive matching technique was used to construct the triangular irregular network surface and white body model. Then, the photos with uniform and consistent attitude and no dislocation were selected to fit on the white body model to obtain the three-dimensional model of the auxiliary facilities. Finally, EPS geographic information workstation is used as vector drawing platform without wearing stereoscopic glasses. Through the built-in drawing module, the outline or frame model of canopy is drawn according to the image and three-dimensional model generated by automatic aerial triangulation. According to the actual needs of the project, select the mark points or special points on the awning, and refer to the actual structure of the line, and then import the EPS data results into AutoCAD software, generate the product model of the ancillary facilities for the use of the construction side.

## 3.4 Route parameter calculation

The core of photogrammetry lies in the planning of the three-dimensional route. The planning plane of the route is parallel to the surface of the object. The form of the route is a bow shape, including the horizontal route and the vertical route.

### 3.4.1 Calculation of horizontal route parameters

To reconstruct the geometric relationship between images, it is necessary to ensure that the image has sufficient overlap, including course overlap and side overlap. Course overlap degree refers to the ratio of the overlapping part of adjacent photos along the course direction to the length of the photo. Side overlap degree refers to the ratio of overlapping side lengths of adjacent photos to photo width between adjacent routes [20].

The field of view Angle of the camera is the fixed value of the camera, which determines the ground imaging range corresponding to the field of view of the camera, as shown in Equation 1.

$$G = 2d \times \tan \frac{fov}{2} \quad (1)$$

In the formula:  $G$  is the corresponding ground imaging range;  $d$  is the photographic distance;  $fov$  is the Angle of view of the camera.

Thus, the coverage area of the horizontal direction of the image can be obtained, as shown in Equation 2.

$$G_x = 2d \times \tan \frac{fov_x}{2} \quad (2)$$

In the formula:  $G_x$  is the coverage range of the horizontal direction of the image;  $d$  is the photographic distance;  $fov_x$  is the horizontal field of view Angle of the camera. The overlapping side length in the horizontal direction is calculated as shown in Equation 3.

$$L_x = p_x \times G_x \quad (3)$$

The distance between two exposure points in the horizontal direction is calculated as shown in Equation 4.

$$\Delta S_x = G_x - L_x = (1 - p_x) \times 2d \times \tan \frac{fov_x}{2} \quad (4)$$

In the formula:  $\Delta S_x$  is the distance between two exposure points in the horizontal direction;  $G_x$  is the coverage range of the horizontal direction of the image;  $L_x$  is the length of overlapping sides in the horizontal direction;  $P_x$  is course overlap degree;  $d$  is the photographic distance;  $fov_x$  is the horizontal field of view Angle of the camera.

### 3.4.2 Vertical route parameter calculation

Different from the horizontal route planning, the vertical direction can be divided into two situations according to whether the safe distance between the UAV and the ground is greater than the elevation height. One is that the minimum safe flight height of the UAV is less than the elevation height. The other is that the minimum safe flight height of UAV is greater than the elevation height.

When the minimum safe flight height  $H_0$  of UAV is less than the elevation height  $H_v$ , Similar to horizontal planning, starting at  $H_0$ . The coverage of the camera is calculated every time the altitude of the aircraft is increased by  $\Delta h$ , until it stops at a time when the coverage exceeds the elevation of the facade. The camera lens is always perpendicular to the elevation, where  $\Delta h$  is calculated as shown in Equation 5.

$$\Delta h = (1 - p_y) \times 2d \times \tan \frac{fov_y}{2} \quad (5)$$

In the formula:  $\Delta h$  is the height between adjacent routes of the UAV;  $p_y$  is the degree of lateral overlap;  $d$  is the photographic distance;  $fov_y$  is the vertical field Angle of the camera [21].

Similarly, the coverage area in the vertical direction of the image can be obtained from Equation (1) and form Equation 6.

$$G_y = 2d \times \tan \frac{fov_y}{2} \quad (6)$$

In the formula:  $G_y$  is the coverage range in the vertical direction of the image;  $d$  is the photographic distance;  $fov_y$  is the vertical field angle of the camera.

The overlapping side length of adjacent photos in the vertical direction is shown in Equation 7.

$$L_y = p_y \times G_y \quad (7)$$

In the formula:  $L_y$  is the overlap length of adjacent photos in the vertical direction;  $p_y$  is the degree of lateral overlap  $G_y$  is the coverage area in the vertical direction of the image.

The distance between two exposure points in the vertical direction is shown in Equation 8.

$$\Delta S_y = G_y - L_y = (1 - p_y) \times 2d \times \tan \frac{fov_y}{2} \quad (8)$$

In the formula:  $\Delta S_y$  is the distance between two exposure points in the vertical direction;  $G_y$  is the coverage area in the vertical direction of the image;  $L_y$  is the overlap length

of adjacent photos in the vertical direction;  $p_y$  is the degree of lateral overlap;  $d$  is the photographic distance;  $dov_y$  is the vertical field Angle of the camera.

In the trajectory planning plane, the elevation values of the exposure points are calculated successively along the vertical direction with an interval of  $\Delta h$  distance.

### 3.5 Close to the technical process of photogrammetry

#### 3.5.1 Data collection

Close photogrammetry follows the principle from coarse to fine. Before route planning, field survey is carried out, oblique photogrammetry or other methods are used to obtain image data of the shot object, and point cloud data of the shot object is obtained through automatic aerial triangulation to generate rough terrain information.

#### 3.5.2 Facade information acquisition

Based on the cloud data, the distance between the safe flight height of the UAV and the elevation as well as the course overlap degree and side overlap degree were set for each elevation planning route according to the actual characteristics of the shooting object and the accuracy requirements of the measurement task.

The integrity of the model is mainly determined by the degree of matching of adjacent elevation images. Image matching is essentially the process of identifying points with the same name between two (or more) images. To ensure that the junction of adjacent facades is better connected and that there are enough points with the same name on the image, during route planning, the route planning plane is extended to both sides appropriately to ensure that the route planning planes of adjacent facades can cross each other. If necessary, the joint between the opposite sides of the drone can also be used to make up the shooting [22].

#### 3.5.3 Data processing and 3D modeling

Due to the influence of weather buildings or other obstacles, the quality of the acquired photos will be affected in different degrees, and there will be great differences in the color and illumination distribution of different photos, which will affect the production and display effect of 3D models. After data collection is completed, check whether the chrominance brightness and contrast of the image meet the requirements to ensure that the image is clear and even in tone. The action recording function in Photoshop is used for batch processing of photos, and brightness saturation and contrast of photos are adjusted to achieve the purpose of uniform light and color. Using Context Capture for data processing, it has powerful data computing capabilities and can restore a millimeter-level model close to the real one. The collected images are added to the software for space-three calculation texture mapping and three-dimensional reconstruction. The software can automatically carry out space-three encryption, calculate the position, attitude angle, and other information of each image, and determine the relative position relationship between the images. By arranging the image control points, the spatial coordinate of the UAV image and the ground close-up image can be unified. Multi-view image matching is the technical basis of automatically generating DSM and constructing 3D models, which can obtain high precision and high-resolution digital surface models. Compared with the traditional single stereo image matching, close photogrammetry can obtain multi-view images and use the redundant information in the images to correct the wrong matching in the photographed ground objects, to ensure the correct matching of the connection points between images [23]. In addition, multi-view images can supplement the features of the ground objects in the shooting blind area that cannot be obtained by traditional means, avoiding the occurrence of the phenomenon of void and pull on the surface of the model. Higher accuracy and more complete texture are closer to the photogrammetry technical process, as shown in Figure 3.

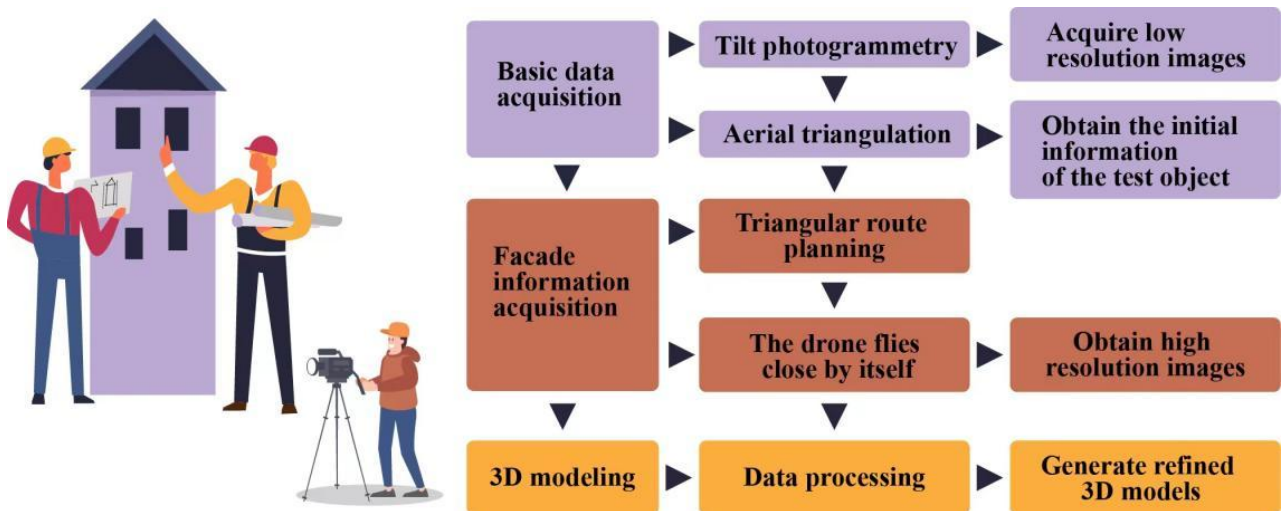


Figure 3: Technique flow chart

### 4 Experimental results and analysis

The object of this experiment is a single building with a relatively open and unobstructed surrounding environment, which is suitable for close photogrammetry operation. The building is low in height and small in area. If inclined photogrammetry is adopted, it is difficult to obtain a fine three-dimensional model of the building. The UAV model is the DJI Phantom 4 Pro. It is a single-lens consumer UAV with relatively low cost, high acquisition efficiency, good mobility performance, and other features. It does not require a high landing site and is suitable for shuttling between urban buildings. The safe flight height of the UAV is lower than the height of the building facade, and the pitch angle of the UAV cradle head is 0, perpendicular to the building facade. The basic data needed for the experiment were obtained by tilt photogrammetry. Due to the low requirement on initial point cloud data for close photogrammetry, three flights of UAV can meet the requirement, and the heading overlap degree and side overlap degree are 80% and 70% respectively. Elevation route planning is mainly based on the UAV platform of Di Da Haotu, and the corresponding flight path is generated through elevation selection parameter setting and other steps. The software carries out route planning for the four facades of the building respectively. According to the different conditions of each facade, different route parameters can be set by changing the corresponding parameters, as shown in Table 1. The data quality of 3D model mainly includes the integrity of the model, position accuracy logical consistency, etc. In order to verify whether the quality of the 3D model produced meets the requirements, it is necessary to evaluate its accuracy. The three-dimensional coordinate values actually measured on the building are compared with the coordinate values of corresponding points with the same name collected on the model. Through comparative analysis, the residual values of X direction, Y direction and Z direction are obtained, and then the error in plane and the error in elevation are obtained. According to the characteristics of experimental objects, the real-time

kinematic (RTK) technology was used in this experiment to acquire field measurement data. Six checkpoints were selected for precision comparison to obtain the statistical error table of checkpoints, as shown in Table 2. It can be seen from the data in Table 2 that the error  $m_x=0.0097m$  in the X direction and  $m_y=0.0110m$  in the y direction of the three-dimensional model obtained close to photogrammetry. The in-plane error  $m_z=0.0111m$  and the in-elevation error  $m_h=0.0130m$  meet the requirements that the in-plane error is less than 0.3m and the in-elevation error is less than 0.5m as stipulated in the 1:500 mapping scale 3D model product of CH/T9015 2012 3D Geographic Information Model Data product specification. The research and simulation of the single building pay more attention to the size, structure and texture information of the building itself, so the relative accuracy is also an important standard to evaluate the quality of the three-dimensional model. The produced 3D model is imported into EPS, and the measured values of the internal model are compared with the measured values of the field industry. The comparison results are expressed in the form of absolute values. The comparison results of eight field-measured plane distance values and eight elevation values between field-measured plane distance values and interior model measured values are shown in Figure 4, and the comparison of elevation values is shown in Figure 5. As can be seen from figure 4 and figure 5, the difference between plane distance measurements and model measurements is 0.006m at maximum and 0.003m at minimum; The difference between the height measurement and the model measurement is 0.005m at the maximum and 0.002m at the minimum, and the accuracy is kept at the level of mm. The geometric accuracy is high and meets the requirements of relevant measurement specifications [24]. The comparative analysis presented in Figure 6, highlights the superior performance of the proposed model across various key indices when compared to existing studies. The proposed model achieves a commendable accuracy of 95%, surpassing the alternatives.

Table 1: Setting of air route parameters

Opposition	Safe flight altitude / m	Distance from the wall wall / m	Heading overlap degree / (%)	Parateral overlap / (%)	Ttai pitch angle
East	0.5	5	70	40	0
West	0.5	5	70	40	0
South	0.5	5	70	40	0
North	0.5	5	70	40	0

Table 2: Checkpoint error statistics table

Number	Model-coordinate Measurement values			Actual coordinate Measurement value			Residual value		
	X	Y	Z	X	Y	Z	$\Delta X$	$\Delta Y$	$\Delta Z$
1	58153.527	3789867.503	382.086	588153.532	3789867.514	382.075	-0.005	-0.011	0.011
2	588157.010	3789867.571	382.116	588157.018	3789867.572	382.098	-0.008	-0.001	0.018
3	588157.130	3789860.797	382.096	588157.116	3789860.785	382.108	0.014	0.012	-0.012
4	588153.619	3789860.674	382.099	588153.608	3789860.659	382.116	0.011	0.015	-0.017
5	588152.725	3789860.763	382.121	588152.713	3789860.771	382.117	0.012	-0.008	0.004
6	588152.690	3789867.411	382.133	588152.703	3789867.424	382.146	-0.013	-0.013	-0.013

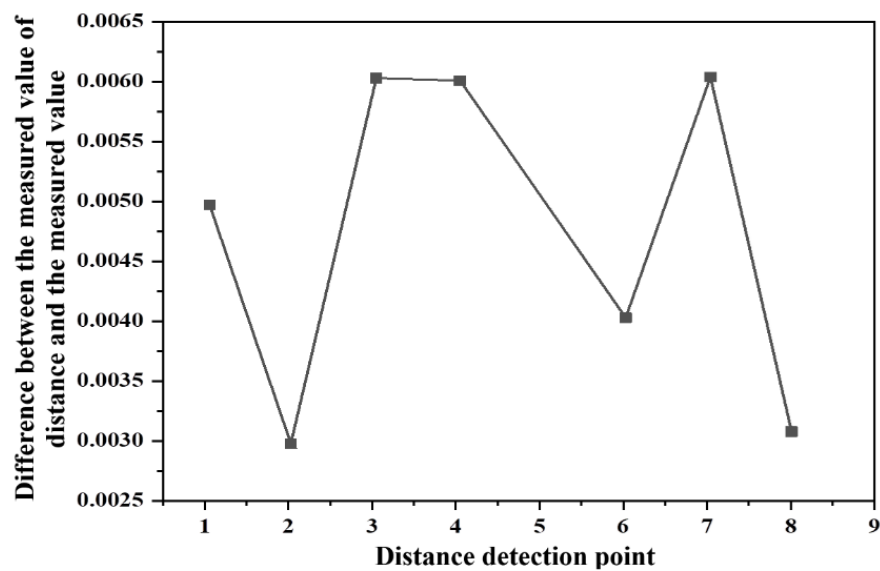


Figure 4: Comparison of the difference between measured and measured distance values

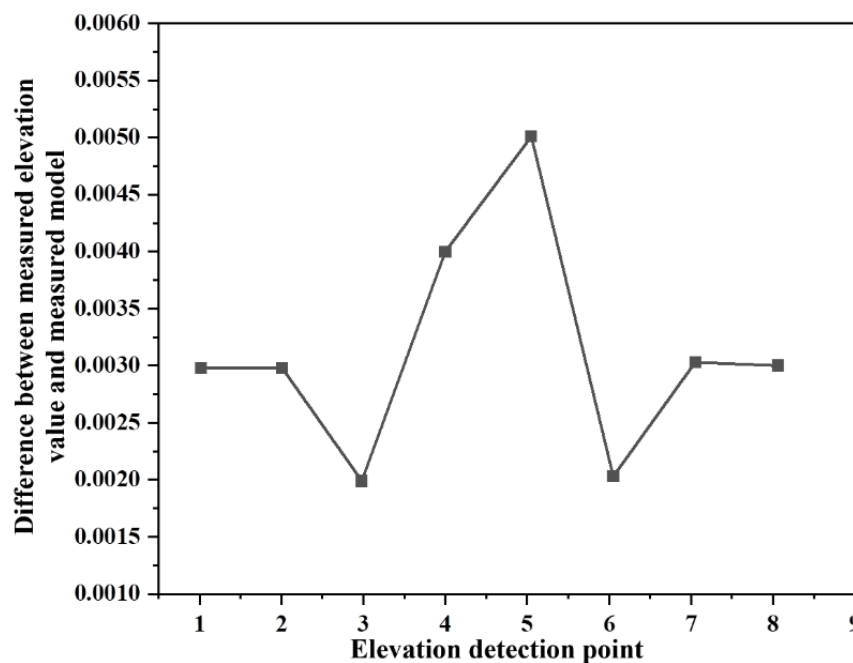


Figure 5: Comparison of difference between measured and measured elevation values



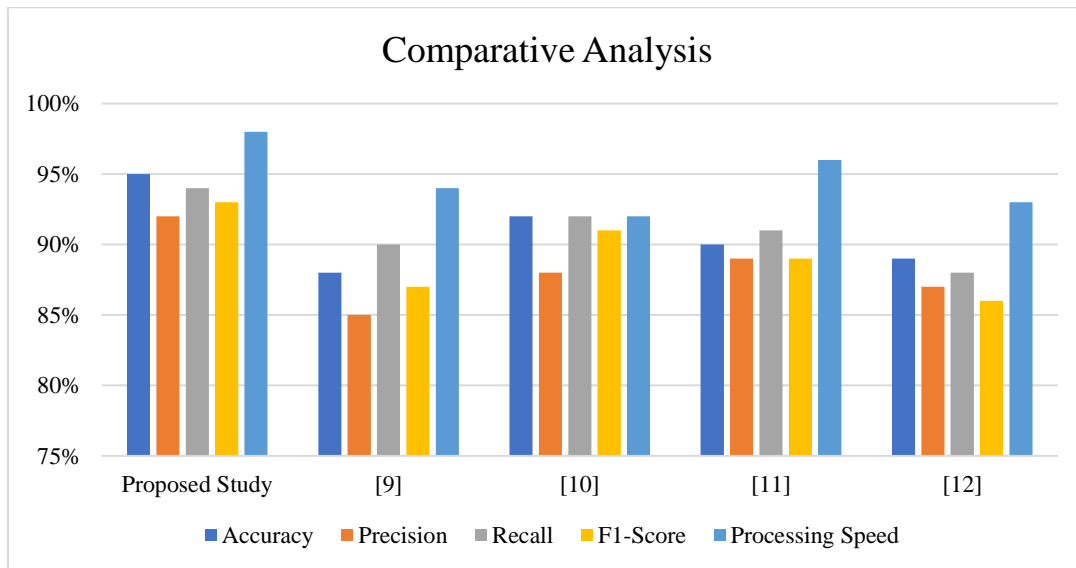


Figure 6: Comparative analysis of proposed study with existing studies [9-12]

Precision, recall, and F1 scores also exhibit strong performance, with values of 92%, 94%, and 93%, respectively. Additionally, the proposed model demonstrates remarkable processing speed at 98%, outperforming all its counterparts. These results collectively underscore the efficacy of the proposed model in terms of accuracy, precision, recall, F1 score, and processing speed. The findings suggest that the proposed model presents a robust solution, showcasing its potential for enhanced efficiency and effectiveness in comparison to existing studies.

## 5 Conclusion

The consumer UAV, with its compact size, high mobility, and flexibility, has proven to be highly efficient in swiftly collecting image data and establishing accurate three-dimensional models. The accuracy of these models aligns seamlessly with relevant standards and specifications, meeting the required criteria for building construction. By implementing UAV tilt photogrammetry technology in combination with complementary software, this study has demonstrated the method's effectiveness in accurately measuring accessory facilities for construction projects. The results not only satisfy stringent accuracy requirements but also significantly enhance overall work efficiency. Field workers benefit from reduced labor intensity and gain a valuable visual reference for the construction of ancillary facilities. Additionally, this technology holds great potential to support a variety of related projects, contributing meaningfully to the development of digital city infrastructure. Future work could explore the integration of advanced sensor technologies, such as LiDAR, and further refine UAV tilt photogrammetry techniques to improve both precision and application scope in building modeling and construction measurement. Moreover, investigating automated post-processing workflows may enhance operational efficiency and scalability in complex construction environments.

## References

- [1] Zhang, P., Xiao, Y., Chen, G., Jiming, E., Li, T., & He, S. (2021, July). Application of oblique photogrammetry in intelligent transportation system. In *Journal of Physics: Conference Series* (Vol. 1972, No. 1, p. 012115). IOP Publishing.
- [2] Wen, Y. (2021). Research on the intelligent construction of prefabricated building and personnel training based on BIM5D. *Journal of Intelligent & Fuzzy Systems*, 40(4), 8033-8041.
- [3] Wang, C., Yu, Q., Law, K. H., McKenna, F., Stella, X. Y., Taciroglu, E., & Cetiner, B. (2021). Machine learning-based regional scale intelligent modeling of building information for natural hazard risk management. *Automation in Construction*, 122, 103474.
- [4] Anisah, A., Ramadhan, M. A., & Haniyyah, S. N. (2022). Development of e-module for construction management application course based on building information modeling. *Rekayasa: Jurnal Penerapan Teknologi dan Pembelajaran*, 19(2), 75-88.
- [5] Massone, L. M., Bedecarratz, E., Rojas, F., & Lafontaine, M. (2021). Nonlinear modeling of a damaged reinforced concrete building and design improvement behavior. *Journal of Building Engineering*, 41, 102766.
- [6] Yang, B., Zhang, B., Zhang, Q., Wang, Z., Dong, M., & Fang, T. (2022). Automatic detection of falling hazard from surveillance videos based on computer vision and building information modeling. *Structure and Infrastructure Engineering*, 18(7), 1049-1063.
- [7] Jasim, N. A., Aljumaily, H. S., Varouqa, I. F., & Al-Zwainy, F. M. (2020). Building information modeling and building knowledge modeling in project management. *Computer Assisted Methods in Engineering and Science*, 28(1), 3-16.
- [8] Liu, K., Wu, H., Ji, Y., & Zhu, C. (2022). Archaeology and restoration of costumes in tang

- tomb murals based on reverse engineering and human-computer interaction technology. *Sustainability*, 14(10), 6232.
- [9] Jang, A., Ju, Y. K., & Park, M. J. (2022). Structural stability evaluation of existing buildings by reverse engineering with 3D laser scanner. *Remote Sensing*, 14(10), 2325.
- [10] Bartonek, D., & Buday, M. (2020). Problems of creation and usage of 3D model of structures and their possible solution. *Symmetry*, 12(1), 181.
- [11] Camagni, F., Colaceci, S., & Russo, M. (2019). Reverse modeling of cultural heritage. Pipeline and bottlenecks. *International Archives of the Photogrammetry, Remote Sensing and Spatial Information Sciences*, 42, 197-204.
- [12] Tiwari, N., Gagare, S. W., & Shaikh, A. A. (2021). Shape recovery analysis of the additive manufactured 3D smart surfaces through reverse engineering. *Progress in Additive Manufacturing*, 6, 281-295.
- [13] Liu, X., He, C., Zhao, H., Jia, J., & Liu, C. (2021). Building information modeling indoor path planning: A lightweight approach for complex BIM building. *Computer Animation and Virtual Worlds*, 32(3-4), e2014.
- [14] Lian, M., & Liu, X. (2022). Significance of building information modeling in modern project management for sustainable smart city applications. *Journal of Interconnection Networks*, 22(Supp01), 2141007.
- [15] Zhang, H., Zhou, J., & Wu, X. (2021). An evolutionary algorithm for non-destructive reverse engineering of integrated circuits. *Computer Modeling in Engineering & Sciences*, 127(3), 1151-1175.
- [16] Pesaran, A., Kim, G. H., Smith, K., Santhanagopalan, S., & Lee, K. J. (2012). *Overview of Computer-Aided Engineering of Batteries and Introduction to Multi-Scale, Multi-Dimensional Modeling of Li-Ion Batteries (Presentation)* (No. NREL/PR-5400-54425). National Renewable Energy Lab. (NREL), Golden, CO (United States).
- [17] Al-Huwaidi, J. S., Al-Obaidi, M. A., Jarullah, A. T., Kara-Zaitri, C., & Mujtaba, I. M. (2021). Modeling and simulation of a hybrid system of trickle bed reactor and multistage reverse osmosis process for the removal of phenol from wastewater. *Computers & Chemical Engineering*, 153, 107452.
- [18] Cheula, R., & Maestri, M. (2022). Nature and identity of the active site via structure-dependent microkinetic modeling: An application to WGS and reverse WGS reactions on Rh. *Catalysis Today*, 387, 159-171.
- [19] Shah, G. A., Polette, A., Pernot, J. P., Giannini, F., & Monti, M. (2022). User-driven computer-assisted reverse engineering of editable CAD assembly models. *Journal of Computing and Information Science in Engineering*, 22(2), 021014.
- [20] Gonzalez-Perez, I., & Fuentes-Aznar, A. (2022). Reverse engineering of spiral bevel gear drives reconstructed from point clouds. *Mechanism and Machine Theory*, 170, 104694.
- [21] Yu, X. (2021, February). Talking about the Application of Computer Reverse Engineering Concept in Sculpture Practice. In *Journal of Physics: Conference Series* (Vol. 1744, No. 2, p. 022082). IOP Publishing.
- [22] Zhang, F., Chan, A. P., Darko, A., Chen, Z., & Li, D. (2022). Integrated applications of building information modeling and artificial intelligence techniques in the AEC/FM industry. *Automation in Construction*, 139, 104289.
- [23] Abate, A. F., Cimmino, L., Cuomo, I., Di Nardo, M., & Murino, T. (2022). On the impact of multimodal and multisensor biometrics in smart factories. *IEEE Transactions on Industrial Informatics*, 18(12), 9092-9100.
- [24] Liu, J., Cao, Y., Xue, Y., Li, D., Feng, L., & Chen, Y. F. (2021). Automatic unit layout of masonry structure using memetic algorithm and building information modeling. *Automation in Construction*, 130, 103858.